Computational Materials Science 99 (2015) 164–172

Contents lists available at ScienceDirect

Computational Materials Science

journal homepage: www.elsevier.com/locate/commatsci

Nonlinear subharmonic oscillation of orthotropic graphene-matrix composite

E. Jomehzadeh [a,*], A.R. Saidi [b], Z. Jomehzadeh [c], F. Bonaccorso [d], V. Palermo [e,f], C. Galiotis [g,h], N.M. Pugno [i,j,k,*]

[a] Department of Mechanical Engineering, Graduate University of Advanced Technology, Kerman, Iran
[b] Department of Mechanical Engineering, Shahid Bahonar University of Kerman, Kerman, Iran
[c] Department of Medical Physics, School of Medicine, Kerman University of Medical Sciences, Kerman, Iran
[d] Istituto Italiano di Tecnologia, Graphene Labs, Genova, Italy
[e] ISOF – Istituto per la Sintesi Organica e la Fotoreattività, Consiglio Nazionale delle Ricerche, Bologna, Italy
[f] Laboratorio MIST.E-R Bologna, Bologna, Italy
[g] Department of Materials Science, University of Patras, Rio Patras, Greece
[h] Institute of Chemical Engineering Sciences, Foundation of Research and Technology-Hellas, Platani, Patras Acahaias, Greece
[i] Laboratory of Bio-Inspired & Graphene Nanomechanics, Department of Civil, Environmental and Mechanical Engineering, Università di Trento, Trento, Italy
[j] Center for Materials and Microsystems, Fondazione Bruno Kessler, Povo (Trento), Italy
[k] School of Engineering & Materials Science, Queen Mary University of London, London, UK

ARTICLE INFO

Article history:
Received 26 August 2014
Received in revised form 16 December 2014
Accepted 20 December 2014

Keywords:
Nonlinear vibration
Subharmonic oscillation
Graphene

ABSTRACT

We investigate the nonlinear responses of graphene-matrix composite to harmonic and subharmonic resonances. Assuming anisotropic mechanical properties of graphene, we derive size-dependent governing equations of motion for graphene resting on a matrix based on the von Karman hypotheses and nonlocal elasticity theory. Response of graphene oscillation under a uniform pressure is obtained using the averaging method. We study the effects of length scale as well as the presence of the elastic matrix on harmonic and subharmonic oscillations of graphene. Our results reveal that subharmonic oscillation of order 1/3 can occur when the ratio of excitation to natural frequencies exceeds three. Also, the subharmonic oscillation of the system is triggered in an appropriate initial condition.

1. Introduction

Graphene is a one-atom-thick sheet of carbon atoms with outstanding electrical [1], mechanical [2], thermal [3] and optical [4] properties. Indeed, graphene has mobility of charge carriers up to $10^6\ cm^2\ V^{-1}\ s^{-1}$ (in suspended samples) [5], Young modulus of 1100 GPa [2], fracture strength of 125 GPa [2], thermal conductivity of $5 \times 10^3\ W\ m^{-1}\ K^{-1}$ [3] and specific surface area of $2630\ m^2\ g^{-1}$ [6]. Due to high stiffness to density ratio [2], graphene has fundamental resonant frequencies at microscale in the Megahertz range 1–170 MHz [7]. This property combined with recent advances in scaling up production techniques [8] by bottom up [9–12] or top down [13–17] approaches have generated considerable interest in utilizing graphene as nanoscale electromechanical resonators [7,18]. In this context, studying the dynamic response of graphene under various loading conditions is fundamental in understanding and explaining the behavior of such nanoscale resonators, key to achieve smart design.

Since experimental and molecular analyses [19,20] of nanostructures are expensive and time-consuming, there is a great interest [21] in exploiting continuum mechanics for analysis of nanostructures [22]. Continuum mechanics has been widely exploited [23,24] in literature for the linear vibration analysis of graphene and single or multi-wall carbon nanotubes, made by rolling up graphene layer(s), mainly exploiting the nonlocal elasticity theory [25–27]. However, interesting physical phenomena such as jumps, subharmonic, super-harmonic and combination resonances as well as chaos occur also in nanostructures in the presence of nonlinearities. Such physical phenomena cannot be taken into account, and thus explained, by linear models [28]. Indeed, no physical system has linear behavior under external perturbations and hence linear models developed for the understanding of physical systems have intrinsic limitations, *i.e.* if the oscillations of an elastic system result in amplitudes which are not very small with respect to its thickness, then the use of linear model may produce inaccurate results. In general, linear models are applicable only in a

* Corresponding authors.
E-mail addresses: e.jomehzadeh@kgut.ac.ir (E. Jomehzadeh), nicola.pugno@unitn.it (N.M. Pugno).

http://dx.doi.org/10.1016/j.commatsci.2014.12.019
0927-0256/

Notation

A	Modal coefficient	U_S	strain energy
E	Young modulus	U_T	kinetic energy
F	external pressure	U_W	potential energy
k	stiffness coefficient of the elastic substrate	U_1	amplitude of the harmonic oscillation
l_1, l_2	length of graphene in x_1 and x_2 directions	$U_{1/3}$	amplitude of the subharmonic oscillation
l_3	graphene thickness	ε	strain tensor
M	resultant moment	μ	length scale parameter (nonlocal parameter)
N	resultant force	θ	chiral angle
p	external load	ν	Poisson's ratio
p_0	magnitude of the external excitation	ρ	density
P	Modal force coefficient	σ	nonlocal stress tensor
u	displacement of graphene	ω	frequency of the external excitation
U	non-dimensional transverse amplitude of oscillation	ω_{nl}	nonlinear natural frequency of graphene

few cases [28], *i.e.* when the vibration amplitude is smaller than the thickness of the tested material. Thus, to accurately understand the dynamic behavior of a nanostructure under general, especially in magnitude, loading conditions, it is essential to take into account the nonlinear contributions.

In this context, several works have been conducted. In particular, the vibrational responses of a cantilever beam with cracks of different size and location to a harmonic force have been investigated [29], demonstrating how the presence of breathing cracks in a beam results in nonlinear dynamic behavior. Such nonlinear dynamic gives rise to super-harmonics in the response signals spectrum [29]. Molecular dynamics (MD), closed-form elasticity solution and finite element method have been exploited by Xue and Liao [21] to understand the elastic response of a circularly shaped graphene layer under a transverse central load. The authors demonstrated that continuum mechanics can yield predictions close to the ones estimated by molecular mechanics under large deformation for certain loading configurations when modes of deformation are similar [21]. Mismatch in deformation profiles is about 8–9% at a central deflection of graphene [21]. The mismatch reduces to less than 5% when the central deflection increased to a 10-layer thickness [21], for the case of a few-layer graphene (FLG) sample. Quinn et al. [30] studied the dynamic buckling of nanostructure subject to compressive edge loading whose transverse displacements are coupled through nonlinear interactions. It was shown that the buckling instability is significantly affected by the presence of the interaction force as well as the separation of the graphene layers at the boundaries [30]. A theoretical framework of nonlinear continuum mechanics was developed by Lu and Huang [31] for graphene under both in-plane and bending deformation. Graphene shows highly nonlinear deformation and anisotropic properties under finite-strain uniaxial stretch [31]. Duan and Wang [32] studied the deformation of a circularly shaped graphene layer under a central point load by carrying out molecular mechanics and nonlinear plate theory. By properly selecting parameters such as Young's modulus, the von Karman plate theory can provide a remarkably accurate prediction of the graphene behavior under linear and nonlinear bending and stretching [32].

Considering the small scale effect by nonlocal elasticity theory, post-buckling, nonlinear bending and nonlinear vibration analyses were presented for simply supported stiff thin films in thermal environments [33,34]. Moreover, Jomehzadeh et al. [35,36] determined how the van der Waals interaction in FLGs has considerable effects on out of phase frequencies. This result was achieved studying the large amplitude free vibrations of FLGs on an elastic substrate using the nonlocal elasticity theory [35,36].

The nonlinear vibrational properties of graphene were studied using a membrane model [37] demonstrating how the nonlinear fundamental frequency of graphene increases with both the in-plane pretension and initial velocity. The nonlinear equation of motion was considered for graphene by including the stretching effects due to large amplitudes [37]. A nonlinear continuum model for the nonlinear vibration analysis of isotropic FLG was developed in [38], without considering the small scale effect. These authors demonstrated that FLGs are promising high-frequency resonators [38].

Forced vibration analysis of nanotubes has been studied [39–41], while more recent works [42,43] considered the vibration behaviors of bi-dimensional systems under applied load. Aksencer and Aydogdu [42] investigated the forced vibration of nanoplates using the nonlocal elasticity theory for all edges simply supported boundary conditions. They have shown that the non-locality effects should be considered for nanoplates under forced vibration [42]. He at al. [43] studied the forced vibration of graphene sheet under a tip force without considering the small scale effects. Exciting a bilayer graphene in proximity of natural frequencies, its first and second layers vibrate in-phase and anti-phase modes, respectively [43].

Since graphene sheets can undergo large displacements within the elastic limit [44], the nonlinear analysis is clearly essential. Here, we theoretically investigate harmonic and subharmonic oscillations of a graphene sheet subjected to harmonic excitation. Large amplitude displacements based on the von Karman theory is assumed. Considering the small scale effect based on the nonlocal elasticity theory [45], the nonlinear governing equations of motion are derived for graphene resting on an elastic foundation. Modal equation is derived exploiting the Galerkin approach. Finally, the response curves of graphene resting on an elastic substrate are presented for both harmonic and subharmonic oscillations. This study could help the dynamical design of graphene-based advanced nonlinear systems.

2. Governing equations

We consider a graphene sheet of dimensions l_1 and l_2 in x_1 and x_2 directions with thickness l_3 [46] rested on an elastic foundation (Fig. 1). The Cartesian coordinate system is fixed at the center of the graphene sheet in its undeformed state. Regarding lateral dimension of graphene sheets, the Kirchhoff hypotheses [47] are applicable. Thus, the displacement components can be represented as

$$u_\alpha = u_\alpha^0 - x_3 u_{3,\alpha}^0, \quad u_3 = u_3^0 \tag{1}$$

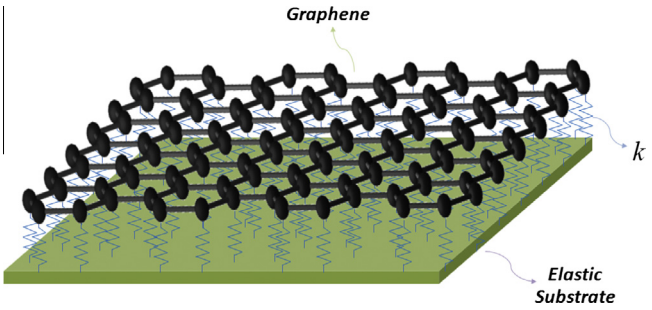

Fig. 1. Schematic representation of graphene sheet resting on an elastic substrate forming a 2D composite.

where $u_i^0 = u_i^0(x_\alpha, t)$ are the displacement components at the middle-plane. A comma stands for differentiation with respect to the suffix index that represents the direction; the Greek subscript (α) can take the numerical value 1 and 2 while the Roman subscript (i) varies from 1 to 3. As the transverse displacement of the graphene sheet u_3^0 becomes comparable to its thickness l_3, the relation between displacement and strain becomes nonlinear. In these conditions, the results obtained by using linear theories are not accurate to describe the strain components. Therefore, a theory of large deflection such as von Karman theory [48] should be used. Indeed, the von Karman theory retains only nonlinear terms that depend on u_3^0. The Green strain components of this theory are expressed as:

$$\varepsilon_{\alpha\beta} = \varepsilon^0_{\alpha\beta} - x_3 u^0_{3,\alpha\beta}, \tag{2}$$

where $\varepsilon^0_{\alpha\beta} = (u^0_{\alpha,\beta} + u^0_{\beta,\alpha} + u^0_{3,\alpha}u^0_{3,\beta})/2$ is the strain component at the center of graphene sheet. The equations of motion can be derived according to the Hamilton's principle as:

$$\delta\Pi = \delta(U_T + U_W - U_S) = 0 \tag{3}$$

where δ is the variational operator and U_T, U_S and U_W are kinetic energy, elastic strain energy of graphene and potential energy of the external loads, respectively. U_T, U_S and U_W are defined by the following relations:

$$U_T = \frac{1}{2}\int_V \rho \ddot{u}_i^2 dV \tag{4a}$$

$$U_S = \frac{1}{2}\int_V \sigma_{\alpha\beta}\varepsilon_{\alpha\beta} dV \tag{4b}$$

$$U_W = \int_A F u_3 dA \tag{4c}$$

where ρ is the density of graphene, σ is the stress component and $F = F(x_\alpha, t)$ is the external pressure, having contribution from both the elastic substrate and applied external forces (p). Substituting Eqs. (1), (2) and (4) into Eq. (3), the equations of motion of graphene are obtained as:

$$N_{\alpha\beta,\beta} = I_1\ddot{u}^0_\alpha - I_2\ddot{u}^0_{3,\alpha} \tag{5a}$$

$$M_{\alpha\beta,\alpha\beta} + (N_{\alpha\beta}u^0_{3,\alpha})_{,\beta} + F = I_1\ddot{u}^0_3 + I_2\ddot{u}^0_{\alpha,\alpha} - I_3\ddot{u}^0_{3,\alpha\alpha} \tag{5b}$$

where $I_i = \int_{-l_3/2}^{l_3/2} \rho x_3^{i-1} dx_3$ denote the inertia parameters, $N_{\alpha\beta}$ and $M_{\alpha\beta}$ are the force and moment resultants which are defined as:

$$N_{\alpha\beta} = \int_{-l_3/2}^{l_3/2} \sigma_{\alpha\beta} dx_3, \quad M_{\alpha\beta} = \int_{-l_3/2}^{l_3/2} \sigma_{\alpha\beta} x_3 dx_3 \tag{6}$$

In order to describe the long range inter-atomic interactions in nanoscale materials and express the results in term of physical parameters, *i.e.* dimensions, the theory of nonlocal elasticity [45] can be used. This theory was first extensively developed since the seventies especially for crack analysis [49]. The theory states that the stress at a certain point in a body depends not only on the classical local strain at that particular location, but also on the spatial integrals with weighted averages of the local strain contribution over all other positions in the body [49]. Therefore, the nonlocal constitutive equations have the following form:

$$\sigma_{\alpha\beta}(x) = C_{\alpha\beta\gamma\lambda}\varepsilon_{\gamma\lambda} + \int_{C_{\alpha\beta\gamma\lambda}(x,x')} \varepsilon_{\gamma\lambda}(x')dx' \tag{7}$$

Since the nonlocal stress components $\sigma_{\alpha\beta}$ are related to Green strain components by an integral form, the governing equations are expressed in integro-differential equations. Since its development, the nonlocal elasticity theory received relatively less attention [24]. This scarce interest in the exploitation of the nonlocal elasticity theory can be attributed to the complexity of the nonlocal stress expression, reported as an integral function of the classical stress over the entire volume of the body. Indeed, the exact or approximate solution for the nonlocal integral function can be determined in very special circumstances using the Green function and hence its use is rather limited. Ref. [45] presented an equivalent differential expression, instead of the integral form, for the nonlocal stress components as:

$$[1 - (e_0a)^2\nabla^2]\sigma_{\alpha\beta}(x) = C_{\alpha\beta\gamma\lambda}\varepsilon_{\gamma\lambda}(x) \tag{8}$$

where $\mu = (e_0a)^2$ is the nonlocal parameter and accounts for the small scale effect, e_0 is a constant to adjust the present model to the experimental results [24], a is an internal characteristic length such as C–C bond length or wave length, $C_{\alpha\beta\gamma\lambda}$ is the stiffness matrix and ∇^2 is the Laplacian operator. The nonlocal effect is presented through the introduction of a nonlocal length scale (μ) which depends on the material and internal characteristic length [45]. The ratio between nonlocal length scale to structural size goes to zero at macro-scale and hence the nonlocal effect vanishes in the limit of large structures recovering the classical mechanics [24].

It is worth to note that the equations of motion (Eq. (5)) have similar format of the classical thin plate theory [50] that considers membrane forces, with the only difference relying on the force and moments resultants. Indeed, in Eq. (5) force and moment resultants are the nonlocal resultant parameters containing small scale effect, while in the classical thin plate theory [49] they are defined by classical parameters considering $\mu = 0$.

The mechanical properties of graphene sheets in a defined direction depend on the chiral angle thus they are considered orthotropic [51]. If a structure executes predominantly transverse nonlinear vibrations, it undergoes a considerable amount of in-plane deformation with negligible in-plane inertial forces [52]. Hence, it is assumed that the in-plane inertia contributions are negligible [50]. Obtaining the force and moments resultants for an anisotropic graphene sheet, introducing the stress function φ as:

$$N_{11} = \varphi_{,22},\ N_{22} = \varphi_{,11},\ N_{12} = -\varphi_{,12}; \tag{9}$$

and considering the small scale effect, the nonlocal nonlinear governing equations of motion for an orthotropic (having different material properties or strengths in diverse orthogonal directions) graphene sheet on an elastic substrate can be obtained as:

$$\begin{aligned} &D_{11}u^0_{3,1111} + 2(D_{12} + 2D_{33})u^0_{3,1122} + D_{22}u^0_{3,2222} \\ &\quad + (I_1 - I_3)\left[1 - (e_0a)^2\nabla^2\right](\ddot{u}^0_3 + \nabla^2\ddot{u}^0_3) \\ &= \left[1 - (e_0a)^2\nabla^2\right][-ku^0_3 + p] \\ &\quad + \left[1 - (e_0a)^2\nabla^2\right]\left(u^0_{3,11}\varphi_{22} - 2u^0_{3,12}\varphi_{12} + u^0_{3,22}\varphi_{11}\right) \end{aligned} \tag{10a}$$

$$A_{11}\varphi_{,1111}+2(A_{12}+2A_{33})\varphi_{,1122}+A_{22}\varphi_{,2222}=u^0_{3,12}u^0_{3,12}-u^0_{3,11}u^0_{3,22} \quad (10b)$$

where the parameters A_{ij} and D_{ij} are the material constants of the graphene sheet, see Appendix A for their definitions, k is the stiffness coefficient of the elastic substrate, which can be considered as the van de Waals pressure coefficient, while p is the external load on the graphene surface.

The governing equations (Eq. (10)) are two nonlinear partial differential equations expressed in terms of the transverse deflection and stress function. Mathematically, the contribution of the elastic substrate is considered by assuming that the reaction of the foundation or substrate can be described by mutually independent spring elements, *i.e.* ku^0_3 is the reaction pressure exerted by an elastic substrate such as a polymer medium.

3. Forced vibration analysis

Let us consider the large amplitude forced vibration analysis of graphene with all four edges simply supported (SSSS) or clamped (CCCC) boundary conditions. In these cases, both harmonic oscillation and subharmonic oscillation of order one third (1/3) are studied. The conditions for simply supported and clamped boundaries can be written as:

$$\text{SSSS}: u^0_3=M_{11}=\varphi_{,12}=\int_{-l_2/2}^{l_2/2}\varphi_{,22}\,dx_2=0 \quad \text{CCCC}: u^0_3=u^0_{3,1}$$
$$=\varphi_{,12}=\int_{-l_2/2}^{l_2/2}\varphi_{,22}\,dx_2=0 \quad \text{at} \quad x_1=\pm\frac{l_1}{2}$$

$$\varphi=\frac{l_3^2\left(Q_{11}Q_{22}-Q_{12}^2\right)}{32n^2m^2l_1^2l_2^2}\cdot\left(\frac{m^4l_1^4\cos(2n\pi x_1/l_1)}{Q_{11}}+\frac{n^4b^4\cos(2m\pi x_2/l_2)}{Q_{22}}\right)U^2(t) \quad (13a)$$

CCCC case

$$\varphi=\frac{l_3^2(Q_{11}Q_{22}-Q_{12}^2)}{32n^2m^2l_1^2l_2^2}\cdot\left(\frac{m^4l_1^4\cos(2n\pi x_1/l_1)}{16Q_{11}}+\frac{m^4l_1^4\cos(4n\pi x_1/l_1)}{16Q_{11}}+\frac{n^4l_2^4\cos(2m\pi x_2/l_2)}{16Q_{22}}+\frac{n^4l_2^4\cos(4m\pi x_2/l_2)}{16Q_{22}}\right)U^2(t)$$
$$+\frac{l_3^2(Q_{11}Q_{22}-Q_{12}^2)}{64}\left(\frac{2Q_{33}(\cos(2n\pi x_1/l_1+2m\pi x_2/l_2)+\cos(-2n\pi x_1/l_1+2m\pi x_2/l_2))}{-2Q_{12}Q_{33}+m^2l_1^2Q_{11}Q_{33}/n^2l_2^2+n^2l_2^2Q_{22}Q_{33}/m^2l_1^2-Q_{12}^2+Q_{11}Q_{22}}\right)U^2(t)$$
$$+\frac{l_3^2}{64}\left(\frac{Q_{33}(\cos(2n\pi x_1/l_1+4m\pi x_2/l_2)+\cos(-2n\pi x_1/l_1+4m\pi x_2/l_2))}{-8Q_{12}Q_{33}+m^2l_1^2Q_{11}Q_{33}/n^2l_2^2+16n^2l_2^2Q_{22}Q_{33}/m^2l_1^2-4Q_{12}^2+4Q_{11}Q_{22}}\right)U^2(t)$$
$$\times\frac{l_3^2}{64}\left(\frac{A_{33}(\cos(4n\pi x_1/l_1+2m\pi x_2/l_2)+\cos(-4n\pi x_1/l_1+2m\pi x_2/l_2))}{-8Q_{12}Q_{33}+16m^2l_1^2Q_{11}Q_{33}/n^2l_2^2+n^2l_2^2Q_{22}Q_{33}/m^2l_1^2-4Q_{12}^2+4Q_{11}Q_{22}}\right)U^2(t) \quad (13b)$$

where Q_{ij} are the coefficients in terms of the material properties (*e.g.* Young's modulus, Poisson's ratio and chiral angle) of the graphene sheets and are defined in Appendix A. Eqs. (13a) and (13b) satisfy in-plane boundary conditions of Eq. (11). Using Eqs. (12) and Eq. (13) and applying Galerkin's technique [53] to Eq. (10a), one can obtain a single, nonlinear, second order differential equation in the form of:

$$\frac{d^2U(t)}{dt^2}+A_1U(t)+A_2U^3(t)=P\cos(\omega t) \quad (14)$$

where A_1 and A_2 are modal coefficients, while P is the modal force coefficient which are expressed in Appendix B.

Putting the external load equal to zero, the nonlinear natural frequency of a square graphene ($l_1=l_2=l$) can be expressed as

$$\omega_{nl}^2=A_1+3/4A_2U^2$$
$$=\frac{16\pi^4Q_{11}Q_{22}(Q_{11}+Q_{22}+2Q_{12}+4Q_{33})+192Q_{11}Q_{22}\frac{l^4}{l_3^4}(1+2\pi^2\mu/l^2)k+9\pi^4(Q_{11}+Q_{22})(Q_{11}Q_{22}-Q_{12}^2)(1+2\pi^2\mu/l^2)U^2}{\rho Q_{11}Q_{22}l^2(\pi^2+6l^2/l_3^2)(1+2\pi^2\mu/l^2)} \quad (15)$$

$$\text{SSSS}: u^0_3=M_{22}=\varphi_{,12}=\int_{-l_1/2}^{l_1/2}\varphi_{,11}\,dx_1=0 \quad \text{CCCC}: u^0_3$$
$$=u^0_{3,2}=\varphi_{,12}=\int_{-l_1/2}^{l_1/2}\varphi_{,11}\,dx_1=0 \quad \text{at} \quad x_2=\pm\frac{l_2}{2} \quad (11)$$

It is assumed that a periodic external pressure $p=p_0\cos(\omega t)$ is applied to the top side of the graphene surface. The parameters ω and p_0 represent the frequency and magnitude of the external excitation load, respectively. The possible solutions of the transverse displacement can be searched in the following form:

$$u^0_3=l_3U(t)\psi(x_\alpha) \quad (12)$$

where U is the non-dimensional transverse amplitude of oscillation. The space function of the transverse displacement can be assumed as $\psi=\cos\left(\frac{n\pi x_1}{l_1}\right)\cos\left(\frac{m\pi x_2}{l_2}\right)$ for all edges simply supported and $\psi=\cos^2\left(\frac{n\pi x_1}{l_1}\right)\cos^2\left(\frac{m\pi x_2}{l_2}\right)$ for all edges clamped of the graphene sheet. Here, n and m represent mode shape number in x_1 and x_2 directions, respectively. Substituting Eq. (12) into Eq. (10b), the general solutions of stress function φ can be obtained as:

SSSS case

It can be seen that how the length scale parameter affects the nonlinear frequency of graphene. Eq. (14) is the well-known second order Duffing equation and in general, most of the papers [54] have only considered its harmonic solutions. Permanent oscillations whose frequency is a fraction $1/n$ of that of the applied force can also occur in nonlinear systems [28].

Now we study in detail the harmonic and subharmonic oscillations of graphene sheets resting on an elastic substrate. We do not attempt to present a general solution of the problem for subharmonic response because in this condition there is not a constant term in the excitation and consequently the subharmonic oscillations of order 1/2 do not occur [28]. Rather, one special case which is the first subharmonic oscillation, *i.e.* the subharmonic oscillation of order 1/3, is treated. An approximate solution is obtained by the procedure known as the averaging method [53]. It is assumed that the transverse amplitude of the graphene layer can be developed in the following form:

$$U(t)=U_1(t)\cos(\omega t)+U_{1/3}(t)\cos\left(\frac{\omega t}{3}\right) \quad (16)$$

where U_1 and $U_{1/3}$ are the amplitude of the harmonic and subharmonic oscillations, respectively. Substituting the proposed form of

Table 1
Material properties of graphene.

	l_1 (nm)	l_2 (nm)	l_3 (nm)	E_{11} (TPa)	E_{22} (TPa)	G_{12} (TPa)	ν_{12}	ρ (Kg/m^3)
Zigzag	4.855	4.888	0.154	1.987	1.974	0.857	0.205	5363
Armchair	4.888	4.855	0.156	1.949	1.962	0.846	0.201	5295

Table 2
Comparison of natural frequencies (GHz) of a clamped zigzag monolayer graphene.

	Dimensions			
	10 × 10 nm	10 × 20 nm	20 × 10 nm	20 × 20 nm
MD [55]	27.28	18.47	18.86	6.94
Present ($U = 0$)	27.65	17.21	17.25	6.91

transverse amplitude (16) into the Duffing Eq. (14) leads to the following relations:

$$(36A_1 - 4\omega^2)U_{1/3} + A_2\left(27U_{1/3}^2 + 27U_1U_{1/3} + 54U_1^2\right)U_{1/3} = 0 \tag{17a}$$

$$\left(A_1 + \frac{3A_2U_{1/3}^2}{2} - \omega^2\right)U_1 + \frac{A_2\left(3U_1^3 + U_{1/3}^3\right)}{4} = P \tag{17b}$$

The above relations are the fundamental equations for harmonic and subharmonic (order 1/3) oscillations of graphene. By setting $A_2 = 0$, *i.e.* the linear oscillation, it can be observed that the coefficient of subharmonic oscillation $U_{1/3}$ must be taken zero unless ω assumes the value $\omega = 3\sqrt{A_1}$, where $\sqrt{A_1}$ is the linear natural frequency of the graphene sheet on an elastic substrate. In these conditions, no subharmonic oscillations will occur. However, if ω assumes the value $3\sqrt{A_1}$, then $U_{1/3}$ can take an arbitrary value.

Eq. (17) have solutions with $U_{1/3} = 0$ or $U_{1/3} \neq 0$. The former solution represents the occurrence of only harmonic oscillations, while the latter represents the combination of subharmonic oscillations of order 1/3 and harmonic oscillations. Solving Eq. (17a), the nontrivial solutions of $U_{1/3}$ can be written as

$$U_{1/3} = \pm\frac{-9A_2U_1 + \sqrt{-567A_2^2U_1^2 - 432A_1A_2 + 48A_2\omega^2}}{18A_2} \tag{18}$$

Depending on the sign of A_2, relation (18) represents an ellipse or a hyperbola in a $U_{1/3}$, ω-plane. Due to real solutions of this relation, it can be concluded that the subharmonic oscillation of order 1/3 occurs in nonlinear forced vibration of a graphene sheet in a specific region of frequencies, *i.e.*

$$\omega > 3\sqrt{\frac{21}{16}A_2U_1^2 + A_1} \text{ for } A_2 > 0 \text{ and}$$
$$\omega < 3\sqrt{\frac{21}{16}A_2U_1^2 + A_1} \text{ for } A_2 < 0 \tag{19}$$

Since the graphene sheet basically shows hardening behavior ($A_2 > 0$) [21], the subharmonic oscillation of order 1/3 occurs when the frequency of the applied force is higher than a specific value as can be seen in Eq. (19). In order to specify the occurrence of subharmonic oscillation with respect to length scale, the first relation of Eq. (19) for an isotropic square graphene can be defined as

$$\omega > \frac{3}{8}\pi^2\sqrt{\frac{E\left(128 + 63(1-\nu^2)\left(1 + 2\pi^2\mu/l^2\right)\right)}{\rho l^2(1-\nu^2)(1 + 2\pi^2\mu/l^2)\left(\pi^2 + 6l^2/l_3^2\right)}} \tag{20}$$

where E and ν are Young modulus and Poisson 's ratio of the isotropic graphene. It can be found that the amplitude of subharmonic oscillation increases by increasing the length scale parameter.

Also, when $U_{1/3} = 0$, relation (17a) is identically satisfied while relation (17b) reduces to the harmonic oscillation of the graphene sheet. Therefore, the subharmonic vibration may result through a bifurcation from the harmonic vibration.

Exploiting Eqs. (17b) and (18), the following relation can be obtained between the applied frequency ω and harmonic amplitude U_1

$$\omega^2 = \frac{4A_1U_1 + 3A_2U_1^3 - 4P}{4U_1} \tag{21}$$

Also, eliminating U_1 from Eq. (17a) and using Eq. (17b) leads a relation between applied frequency ω and subharmonic amplitude $U_{1/3}$ as

$$\frac{\left(A_1 + \frac{3A_2U_{1/3}^2}{2} - \omega^2\right)\left(-9U_{1/3}A_2 - \sqrt{96A_2\omega^2 - 567U_{1/3}^2A_2^2 - 864A_1A_2}\right)}{36A_2} + \frac{\left(-9U_{1/3}A_2 - \sqrt{96A_2\omega^2 - 567U_{1/3}^2A_2^2 - 864A_1A_2}\right)^3}{62208A_2^3} + \frac{A_2U_{1/3}^3}{4} = P \tag{22}$$

This equation is simplified in terms of length scale parameter in Appendix C.

4. Numerical results

In order to perform the numerical calculations, two types of graphene sheet with geometric and material properties presented

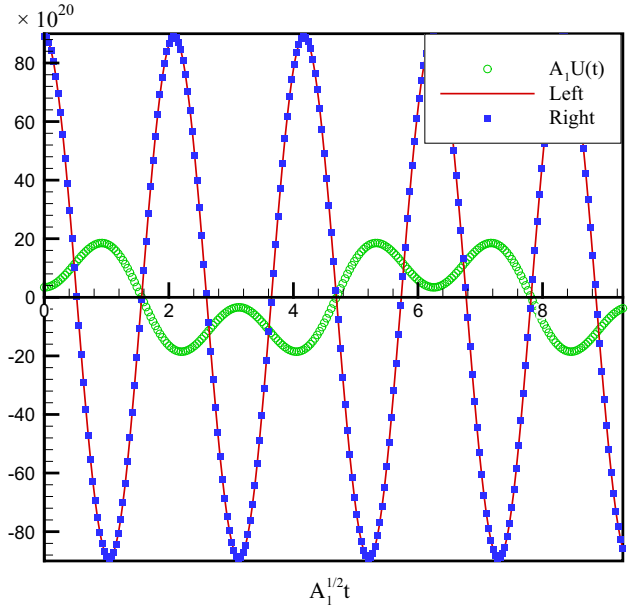

Fig. 2. Comparison of the left and right sides of Eq. (14) for zigzag graphene ($p_0 = 2$ Mpa).

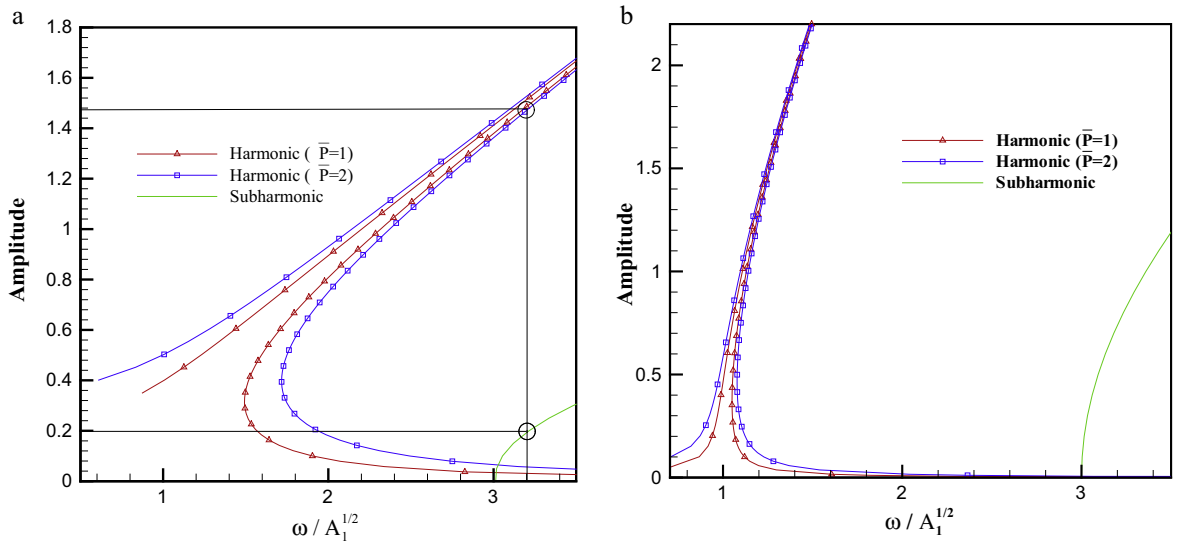

Fig. 3. Harmonic and subharmonic response curves of a graphene sheet with boundary conditions (a) edges simply supported (SSSS), (b) all edges clamped (CCCC).

in Table 1 are considered [33]. Also, the nonlocal parameter and substrate stiffness coefficient are assumed to be $e_0a = 1.5$ nm and $k = 28.49$ GPa/nm, respectively [36].

The obtained natural frequencies for a clamped zigzag monolayer graphene are compared with molecular dynamics (MD) simulation using the REBO potential [55] in Table 2. Since the amplitude of vibration is not mentioned in Ref. [55], we consider the linear case for this comparison.

To ensure the occurrence of the subharmonic oscillation of order 1/3 and the accuracy of its results, the time variation of left side of Eq. (14), in which relation (16) is used for $U(t)$, are compared with the excitation function on the right side of Eq. (14) in which the frequency of the excitation is $\omega = 3\sqrt{A_1}$. The numerical values of left (output results) and right (input data) sides of Eq. (14) are compared in Fig. 2 and it can be found that both sides are in agreement with each other. Based on the results presented in Fig. 2, it can be seen that the response frequency of the graphene sheet is one third of the excitation frequency.

The harmonic and subharmonic response curves of a zigzag graphene sheet are depicted in Fig. 3 for both simply and clamped boundary conditions. The parameter $\overline{P}$ is related to magnitude of excitation as $\overline{P} = p_0 l_1^4 / E_{11} l_3^4$ where E_{11} is the Young's modulus in the direction of chiral vector. The amplitude in figures is U_1 or $U_{1/3}$ for harmonic and subharmonic, respectively which is non-dimensional with respect to the thickness. To better understand the regions of harmonic and subharmonic, the value of amplitude is shown for frequency ratio of 3.2. It can be seen that for this frequency both harmonic and subharmonic oscillation can occur with dimensionless amplitude of nearly 0.2 and 1.44, respectively.

It can be seen that the subharmonic response for both boundary conditions starts from the value $\omega/\sqrt{A_1} = 3$. Moreover, it can be found that since the graphene sheet with simply supported edges

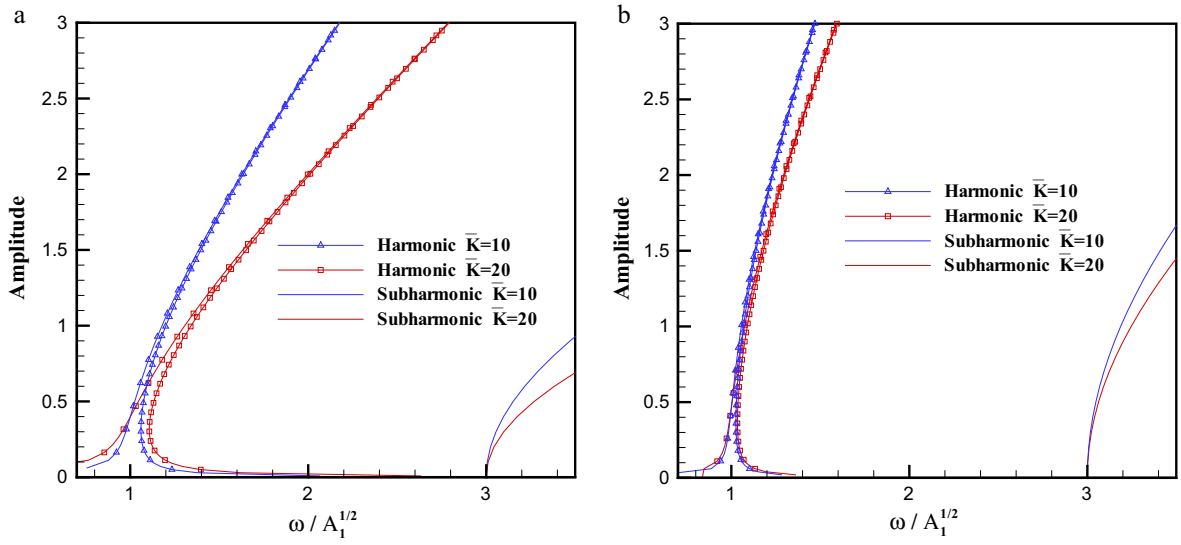

Fig. 4. Effect of elastic foundation on response curves of a zigzag graphene sheet $\overline{K} = \frac{kl_2^4}{E_{11}l_3^4}$ with boundary conditions (a) all edges simply supported (SSSS), (b) all edges clamped (CCCC).

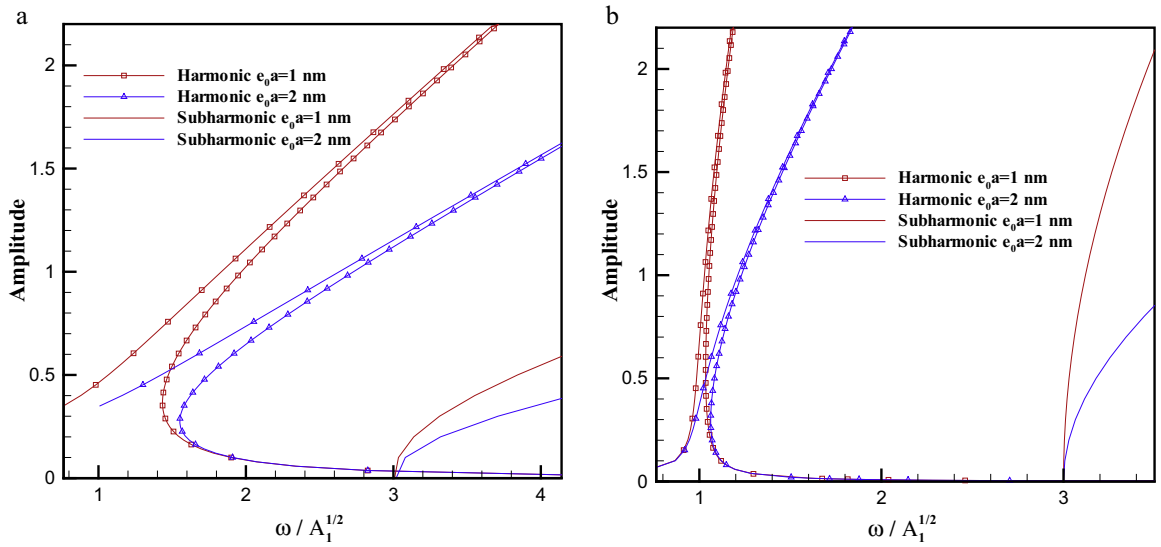

Fig. 5. Effect of nonlocal parameter on response curves of a zigzag graphene with boundary conditions (a) all edges simply supported (SSSS), (b) all edges clamped (CCCC).

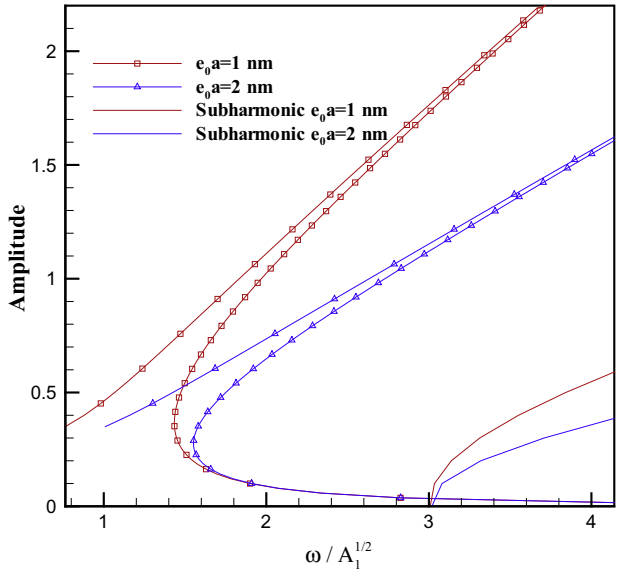

Fig. 6. Response curves of a simply supported armchair graphene for different nonlocal parameters.

has considerable nonlinear behavior, due to its low stiffness with respect to the clamped one, the occurrence of subharmonic response is here more pronounced. Also, it can be found that the harmonic oscillations can also occur in the region of the excitation frequency where the subharmonic oscillations take place and this effect is more considerable for simply supported graphene. Results show that the nonlinear behavior of graphene sheets is of hardening type, i.e., the frequency increases with the amplitude, as expected due to stretching. Since the external force is harmonic, its magnitude does not affect the subharmonic response.

In order to study the effect of elastic substrate on vibrational behavior of graphene sheets, response curves are shown in Fig. 4 for different values of the elastic foundation as a matrix in the 2D composites. It can be found that as the elasticity of the matrix increases, the nonlinear vibrational behavior of graphene sheet decreases and curves shift to left. Therefore, for high stiff elastic substrate, the linear analysis may have acceptable results. Also, it can be seen that the elastic substrate has considerable effect on simply supported graphene than clamped one. Moreover, the effects of substrate are more significant in higher frequencies for both harmonic and subharmonic oscillations. Similar to single layer graphene, it can be seen that the subharmonic response for a graphene-matrix composite also starts from frequency ratio around 3. However, the elastic substrate causes decreasing of subharmonic amplitude.

The response curves of a zigzag graphene sheet are depicted for different values of nonlocal parameter in Fig. 5 for both simply supported and clamped edges. Consequently, there is a strong increase in the nonlinear vibrational behavior and therefore, the nonlinear effects are more considerable for higher values of small length scale. It can be concluded that for nanostructures the use of nonlinear and nonlocal effects are essential for obtaining accurate results. Also, the length scale effect decreases not only the harmonic amplitude but also subharmonic amplitude of graphene.

The response curves of a simply supported armchair graphene sheet are shown in Fig. 6 for some values of nonlocal parameter. By comparing Fig. 6 with Fig. 5a it can be found that the nonlocality has the same effect for both zigzag and armchair graphene, i.e., a length scale effect increment decreases the amplitude of oscillation.

5. Conclusions

Nonlinear forced vibration of a graphene sheet resting on an elastic substrate has been presented by considering the small scale effect. Harmonic as well as subharmonic oscillations have been developed to study the vibrational behavior of an orthotropic graphene sheet. The governing equations of motion have been derived using the von Karman hypotheses. The Galerkin's procedure and method of averaging have been used to reduce the formulations into a modal equation. The responses of the problem have been obtained for two different boundary conditions.

It is concluded that the subharmonic oscillation of order 1/3 can occur in graphene sheets with harmonic excitation. The transition between the state in which the subharmonic oscillation of order 1/3 occurs and the state in which the harmonic oscillation occurs cannot be continuous and only when an appropriate initial condition is given to the system, the subharmonic oscillation is triggered. Our calculations demonstrate that subharmonic oscillations of 1/3 can occur only when the ratio of excitation frequency is more than 3. In this frequency region, harmonic oscillations can also take place

as well. In addition, our results demonstrate that the small length scale has considerable effect on the vibrational behavior of graphene sheets, increasing the nonlinearity of the system.

Acknowledgments

The financial support of Iran Nanotechnology Initiative Council is gratefully acknowledged. NMP is supported by the European Research Council (ERC StG Ideas 2011 BIHSNAM n.279985 on "Bio-Inspired hierarchical super-nanomaterials", ERC PoC 2013-1 REPLICA2 n. 619448 on "Large-area replication of biological anti-adhesive nanosurfaces", ERC PoC 2013-2 KNOTOUGH n. 632277 on "Super-tough knotted fibres"), by the European Commission under the Graphene Flagship (contract number, n. 604391) and by the Provincia Autonoma di Trento ("Graphene Nanocomposites", n. S116/2012-242637 and reg.delib. n. 2266).

Appendix A

The coefficients of the governing equations of motion are obtained in terms of mechanical properties of graphene sheets as

$$A_{11}=\frac{Q_{22}}{l_3(Q_{11}Q_{22}-Q_{12}^2)},\quad A_{12}=-\frac{Q_{12}}{l_3(Q_{11}Q_{22}-Q_{12}^2)},$$
$$A_{22}=\frac{Q_{11}}{l_3(Q_{11}Q_{22}-Q_{12}^2)},\quad A_{33}=\frac{1}{l_3Q_{33}},\tag{A.1}$$
$$D_{11}=\frac{l_3^3Q_{11}}{12},\quad D_{12}=\frac{l_3^3Q_{12}}{12},D_{22}=\frac{l_3^3Q_{22}}{12},\quad D_{33}=\frac{l_3^3Q_{33}}{12}$$

where

$$\begin{aligned}
Q_{11}&=\frac{E_{11}\left(\cos^4\theta+2\nu_{21}\sin^2\theta\cos^2\theta\right)+E_{22}\sin^4\theta}{1-\nu_{12}\nu_{21}}+4G_{12}\sin^2\theta\cos^2\theta\\
Q_{12}&=\frac{E_{11}\left(\sin^2\theta\cos^2\theta+\nu_{21}\sin^4\theta+\nu_{21}\cos^4\theta\right)+E_{22}\sin^2\theta\cos^2\theta}{1-\nu_{12}\nu_{21}}-4G_{12}\sin^2\theta\cos^2\theta\\
Q_{22}&=\frac{E_{11}\left(\sin^4\theta+2\nu_{21}\sin^2\theta\cos^2\theta\right)+E_{22}\cos^4\theta}{1-\nu_{12}\nu_{21}}+4G_{12}\sin^2\theta\cos^2\theta\\
Q_{33}&=\frac{E_{11}\left(\sin^2\theta\cos^2\theta-2\nu_{21}\sin^2\theta\cos^2\theta\right)+E_{22}\sin^2\theta\cos^2\theta}{1-\nu_{12}\nu_{21}}+G_{12}(\cos^2\theta-\sin^2\theta)
\end{aligned}\tag{A.2}$$

where θ denotes the chiral angle [33], E_{11} and E_{22} are Young's modulus in the direction and perpendicular to the chiral vector, respectively. Also, G_{12} and ν are the shear modulus and Poisson's ratio of the graphene sheet, respectively.

Appendix B

The modal coefficients for a simply supported graphene sheet can be obtained as:

$$A_1=\frac{12l_1^2l_2^2(1+\pi^2\mu l_1^2+\pi^2\mu l_2^2)k-\pi^4l_3^3(2Q_{12}l_1^2l_2^2+4Q_{33}l_1^2l_2^2+Q_{22}l_1^4+Q_{11}l_2^4)}{(12l_1^2l_2^2+l_1^2l_3^2\pi^2+l_2^2l_3^2\pi^2)(l_1^2l_2^2+l_1^2\mu\pi^2+l_2^2\mu\pi^2)\rho l_3}\tag{B.1}$$

$$A_2=\frac{3\pi^4l_3^2(l_1^4Q_{22}+l_2^4Q_{11})(Q_{11}Q_{22}-Q_{12}^2)}{4\rho Q_{11}Q_{22}l_1^2l_2^2(12l_1^2l_2^2+l_1^2l_3^2\pi^2+l_2^2l_3^2\pi^2)}\tag{B.2}$$

$$P=\frac{192l_1^4l_2^4}{\rho l_3^2\pi^2\left(12l_1^2l_2^2+\pi^2l_3^2l_2^2+\pi^2l_3^2l_1^2\right)\left(\pi^2\mu l_2^2+\pi^2\mu l_1^2+l_1^2l_2^2\right)}p_0\tag{B.3}$$

where Q_{ij} is defined in Appendix A.

Appendix C

The relation between applied frequency ω and subharmonic amplitude $U_{1/3}$ in term of length scale parameter for a square graphene is

$$\begin{aligned}
&\frac{\left(-9(1-\nu^2)(1+2\pi^2\mu/l^2)U_{1/3}-16l^2-\omega^2\right)\left(-\frac{27}{4}\pi^4El_3^2U_{1/3}-\frac{1}{4}\sqrt{1152\pi^4\rho\omega^2El_3^2l^4(6+\pi^2l_3^2/l^2)-5103\pi^4\rho\omega^2El_3^2l^4(6+\pi^2l_3^2/l^2)l^2(6+\pi^2l_3^2/l^2)U_{1/3}^2-4096l^2}\right)}{27\pi^4El_3^2}\\
&+\left(\frac{\frac{27}{4}\pi^4El_3^2U_{1/3}-\frac{1}{4}\sqrt{1152\pi^4\rho\omega^2El_3^2l^4(6+\pi^2l_3^2/l^2)-5103\pi^4\rho\omega^2El_3^2l^4(6+\pi^2l_3^2/l^2)l^2(6+\pi^2l_3^2/l^2)U_{1/3}^2-4096l^2}}{20\pi^4El_3^2}\right)^3+\frac{9\pi^4El_3^2U_{1/3}^3}{\rho(6+\pi^2l_3^2/l^2)l^4}\\
&=\frac{96l^4p_0}{\rho\pi^2l^4l_3^2(6+\pi^2l_3^2/l^2)(1+2\pi^2\mu/l^2)l^4}
\end{aligned}\tag{C.1}$$

References

[1] A.K. Geim, K.S. Novoselov, Nat. Mater. 6 (2007) 183–191.
[2] C. Lee, X. Wei, J.W. Kysar, J. Hone, Science 321 (2008) 385–388.
[3] A.A. Balandin, S. Ghosh, W. Bao, I. Calizo, D. Teweldebrhan, F. Miao, C.N. Lau, Nano Lett. 8 (2008) 902–907.
[4] F. Bonaccorso, Z. Sun, T. Hasan, A.C. Ferrari, Nat. Photonics 4 (2010) 611–622.
[5] D.C. Elias, R.V. Gorbachev, A.S. Mayorov, S.V. Morozov, A.A. Zhukov, P. Blake, L.A. Ponomarenko, I.V. Grigorieva, K.S. Novoselov, F. Guinea, A.K. Geim, Nat. Phys. 7 (2011) 701–704.
[6] M.D. Stoller, S. Park, Y. Zhu, J. An, R.S. Ruoff, Nano Lett. 8 (2008) 3498–3502.
[7] J.S. Bunch, A.M. van der Zande, S.S. Verbridge, I.W. Frank, D.M. Tanenbaum, J.M. Parpia, H.G. Craighead, P.L. McEuen, Science 315 (2007) 490–493.
[8] F. Bonaccorso, A. Lombardo, T. Hasan, Z. Sun, L. Colombo, A.C. Ferrari, Mater. Today 15 (2012) 564–589.
[9] K.V. Emtsev, A. Bostwick, K. Horn, J. Jobst, G.L. Kellogg, L. Ley, J.L. McChesney, T. Ohta, S.A. Reshanov, J. Röhrl, E. Rotenberg, A.K. Schmid, D. Waldmann, H.B. Weber, T. Seylle, Nat. Mater. 8 (2009) 203–207.
[10] S. Bae, H. Kim, Y. Lee, X. Xu, J.S. Park, Y. Zheng, J. Balakrishnan, T. Lei, H.R. Kim, Y.I. Song, Y.J. Kim, K.S. Kim, B. Özyilmaz, J.H. Ahn, B.H. Hong, S. Iijima, Nat. Nanotechnol. 5 (2011) 574–578.
[11] C. Berger, Z. Song, T. Li, X. Li, A.Y. Ogbazghi, R. Feng, Z. Dai, A.N. Marchenkov, E.H. Conrad, P.N. First, W.A. de Heer, J. Phys. Chem. B 108 (2004) 19912–19916.
[12] X. Li, W. Cai, J. An, S. Kim, J. Nah, D. Yang, R. Piner, A. Velamakanni, I. Jung, E. Tutuc, S.K. Banerjee, L. Colombo, R.S. Ruoff, Science 324 (2009) 1312–1314.
[13] Y. Hernandez, V. Nicolosi, M. Lotya, F.M. Blighe, Z. Sun, S. De, I.T. McGovern, B. Holland, M. Byrne, Y.K. Gun'Ko, J.J. Boland, P. Niraj, G. Duesberg, S. Krishnamurthy, R. Goodhue, J. Hutchison, V. Scardaci, A.C. Ferrari, J.N. Coleman, Nat. Nanotechnol. 3 (2008) 563–568.
[14] A.A. Green, M.C. Hersam, Nano Lett. 9 (2009) 4031–4036.
[15] O.M. Maragó, F. Bonaccorso, R. Saija, G. Privitera, P.G. Gucciardi, M.A. Iatì, G. Calogero, P.H. Jones, F. Borghese, P. Denti, V. Nicolosi, A.C. Ferrari, ACS Nano 4 (2010) 7515–7523.
[16] F. Torrisi, T. Hasan, W. Wu, Z. Sun, A. Lombardo, T.S. Kulmala, G.W. Hsieh, S. Jung, F. Bonaccorso, P.J. Paul, D. Chu, A.C. Ferrari, ACS Nano 6 (2012) 2992–3006.
[17] J. Hassoun, F. Bonaccorso, M. Agostini, M. Angelucci, M.G. Betti, R. Cingolani, M. Gemmi, C. Mariani, S. Panero, V. Pellegrini, B. Scrosati, Nano Lett. 14 (2014) 4901–4906.
[18] J. Atalaya, A. Isacsson, J.M. Kinaret, Nano Lett. 8 (2008) 4196–4200.
[19] P.H. Tan, W.P. Han, W.J. Zhao, Z.H. Wu, K. Chang, H. Wang, Y.F. Wang, N. Bonini, N. Marzari, N. Pugno, G. Savini, A. Lombardo, A.C. Ferrari, Nat. Mater. 11 (2012) 294–300.
[20] X. Shi, N.M. Pugno, Y. Cheng, H. Gao, Appl. Phys. Lett. 95 (2009) 163113.

[21] X. Xu, K. Liao, Mater. Phys. Mech. 4 (2001) 148–151.
[22] E. Jomehzadeh, M.K. Afshar, C. Galiotis, X. Shi, N.M. Pugno, Int. J. Non-Linear Mech. 56 (2013) 123–131.
[23] K.M. Liew, X.Q. He, S. Kitipornchai, Acta Mater. 54 (2006) 4229–4236.
[24] B. Arash, Q. Wang, Comput. Mater. Sci. 51 (2012) 303–313.
[25] C.W. Lim, Q. Yang, J.B. Zhang, Int. J. Non-Linear Mech. 47 (2012) 496–505.
[26] T. Murmu, S.C. Pradhana, J. Appl. Phys. 105 (2009) 064319.
[27] E. Jomehzadeh, A.R. Saidi, Compos. Struct. 93 (2011) 1015–1020.
[28] J.J. Stoker, Nonlinear Vibrations in Mechanical and Electrical Systems, John Wiley & Sons, New York, London, 1950.
[29] N. Pugno, C. Surace, R. Ruotolo, J. Sound Vib. 235 (2000) 749–762.
[30] D.D. Quinn, J.P. Wilber, C.B. Clemons, G.W. Young, A. Buldum, Int. J. Non-Linear Mech. 42 (2007) 681–689.
[31] Q. Lu, R. Huang, Int. J. Appl. Mech. 1 (2009) 443–467.
[32] W.H. Duan, C.M. Wang, Nanotechnology 20 (2009) 075702.
[33] L. Shen, H.S. Shen, C.L. Zhang, Comput. Mater. Sci. 48 (2010) 680–685.
[34] H.S. Shen, Compos. Struct. 93 (2011) 1143–1152.
[35] E. Jomehzadeh, A.R. Saidi, Comput. Mater. Sci. 50 (2011) 1043–1051.
[36] E. Jomehzadeh, A.R. Saidi, N.M. Pugno, Physica E 44 (2012) 1973–1982.
[37] J. Rezaei Mianroodi, S. Amini Niaki, R. Naghdabadi, M. Asghari, Nanotechnology 22 (2011) 305703.
[38] J. Wang, X. He, S. Kitipornchai, H. Zhang, J. Phys. D Appl. Phys. 44 (2011) 135401.
[39] P. Karaoglu, M. Aydogdu, Proc. Inst. Mech. Eng. Part C: J. Mech. Eng. Sci. 224 (2010) 497–503.
[40] P. Soltani, J. Saberian, R. Bahramian, A. Farshidianfar, Int. J. Fundamental Phys. Sci. 1 (2011) 47–52.
[41] M. Simsek, Comput. Mater. Sci. 50 (2011) 2112–2123.
[42] T. Aksencer, M. Aydogdu, Physica E 44 (2012) 1752–1759.
[43] X.Q. He, J.B. Wang, B. Liu, K.M. Liew, Comput. Mater. Sci. 61 (2012) 194–199.
[44] J.W. Jiang, J.S. Wang, B. Li, Phys. Rev. B 81 (2010) 073405.
[45] A.C. Eringen, J. Appl. Phys. 54 (1983) 4703–4710.
[46] Y. Huang, J. Wu, K.C. Hwang, Phys. Rev. B 74 (2006) 245413.
[47] G.R. Kirchhoff, JFuer die Reine und Angewandte Mathematik 40 (1850) 51–88.
[48] T.h. Von Karman, Encyklop die der mathematischen. Wissenschaften (1910) 5–6.
[49] A.C. Eringen, D.G.B. Edelen, Int. J. Eng. Sci. 10 (1972) 233–248.
[50] S. Timoshenko, The Theory of Plates and Shells, McGraw-Hill, 1940.
[51] P.R. Wallace, Phys. Rev. 71 (1947) 622–634.
[52] C.P. Vendhan, Y.C. Das, J. Sound Vib. 39 (1975) 147–157.
[53] A. Ern, J.L. Guermond, Theory and Practice of Finite Elements, Springer, 2004, ISBN 0-387-20574-8.
[54] A.H. Nayfeh, D.T. Mook, Nonlinear Oscillations, John Wiley & Sons, New York, 1995.
[55] A. Shakouri, T.Y. Ng, R.M. Lin, Nanotechnology 22 (2011) 469502.